Microsc. Microanal. 9, 74–85, 2003
DOI: 10.1017/S1431927603030046

Microscopy AND Microanalysis



# Simultaneous Mechanical Loading and Confocal Reflection Microscopy for Three-Dimensional Microbiomechanical Analysis of Biomaterials and Tissue Constructs

Sherry L. Voytik-Harbin,[1,2]* Blayne A. Roeder,[3] Jennifer E. Sturgis,[1] Klod Kokini,[2,3] and J. Paul Robinson,[1,2]

[1]*Department of Basic Medical Sciences, Purdue University, 1515 Hansen Hall, West Lafayette, IN 47907-1515, USA*
[2]*Department of Biomedical Engineering, Purdue University, West Lafayette, IN 47907-1296, USA*
[3]*School of Mechanical Engineering, Purdue University, West Lafayette, IN 47907-1288, USA*

**Abstract:** At present, mechanisms by which specific structural and mechanical properties of the three-dimensional extracellular matrix microenvironment influence cell behavior are not known. Lack of such knowledge precludes formulation of engineered scaffolds or tissue constructs that would deliver specific growth-inductive signals required for improved tissue restoration. This article describes a new mechanical loading–imaging technique that allows investigations of structural–mechanical properties of biomaterials as well as the structural–mechanical basis of cell–scaffold interactions at a microscopic level and in three dimensions. The technique is based upon the integration of a modified, miniature mechanical loading instrument with a confocal microscope. Confocal microscopy is conducted in a reflection and/or fluorescence mode for selective visualization of load-induced changes to the scaffold and any resident cells, while maintaining each specimen in a "live," fully hydrated state. This innovative technique offers several advantages over current biomechanics methodologies, including simultaneous visualization of scaffold and/or cell microstructure in three dimensions during mechanical loading; quantification of macroscopic mechanical parameters including true stress and strain; and the ability to perform multiple analyses on the same specimen. This technique was used to determine the structural–mechanical properties of three very different biological materials: a reconstituted collagen matrix, a tissue-derived biomaterial, and a tissue construct representing cells and matrix.

**Key words:** confocal reflection microscopy, extracellular matrix, biomaterials, mechanical properties, biomechanics, three-dimensional, microstructure, micromechanics

## Introduction

Understanding how the cellular response proceeds within the three-dimensional context of structural and mechanical restraints offered by the extracellular matrix (ECM) will drive the next generation of engineered scaffolds (biomaterials) and devices to be used for repair and replacement of defective tissues. It is now well accepted that the complex three-dimensional structural–mechanical environment of cells *in vivo*, including time-varying changes in stresses and strains, significantly influences the fundamental cellular re-

Received January 31, 2001; accepted May 2, 2002.
*Corresponding author. E-mail: voytik@ecn.purdue.edu

sponse in terms of cell morphology, phenotype, and function (Galbraith and Sheetz, 1998; Ingber, 1998; Chiquet, 1999; Cowin, 2000). Therefore, it is likely that the ability of an engineered biomaterial or tissue construct to approximate the structural–mechanical aspects of the cellular microenvironment is an important factor in determining the eventual success or failure of such engineered devices when used clinically for tissue repair or replacement. Unfortunately, the critical structural and mechanical parameters of the cellular microenvironment necessary for the establishment and maintenance of tissue form and function have yet to be identified and prioritized. Likewise, the detailed mechanisms involved in the transmission of mechanical forces between the cell and its supporting extracellular scaffold (i.e., mechanotransduction) remain to be elucidated. One of the major difficulties in defining these structural–mechanical aspects that are fundamental to cell–scaffold interactions is the inability to precisely characterize, either qualitatively or quantitatively, the structural composition and mechanical properties (stress and strain states) of the three-dimensional microenvironment in which cells reside.

Although a number of techniques have to date been developed to investigate structural–mechanical relationships of tissue explants and simulated tissue constructs at macroscopic, microscopic, and molecular levels of function, each method has its limitations. The most traditional method involves application of a mechanical load to a specimen, fixation of the specimen under load, and examination of the structural characteristics of the cells and/or the supporting scaffold or matrix via routine light and electron microscopy techniques (Viidik, 1972; Eastwood et al., 1998; Lee et al., 2000). For example, Eastwood and coworkers (1998) evaluated fixed specimens using both stereomicroscopy and scanning electron microscopy (SEM) to determine the effect of cyclic loading on fibroblast shape and alignment within collagenous matrices. Disadvantages of these routine light or electron microscopy techniques for biomechanics studies include the inability to perform multiple observations within a single specimen in a native or "live" state and visualization in two rather than three dimensions. Additionally, specimen preparation techniques required for these imaging methods, including fixation, critical-point drying, and application of conductive coating, often create significant artifacts in the microstructure (Ottani et al., 2001). Attempts to minimize specimen processing for collection of more accurate microstructural information have included the application of an environmental SEM. Specifically, studies involving the structural–mechanical properties of collagen–glycosaminoglycan analogues of the ECM have shown that while use of the environmental SEM did eliminate the need for conductive coating of specimens, these specimens still required freeze drying or critical-point drying since water interfered with imaging of the collagen fibrils (Chen et al., 1995).

Other methods have been developed that allow structural analyses of cells and/or scaffolds within mechanically loaded specimens maintained in a native, hydrated state. Laser Raman microscopy (Wang et al., 2000), and Synchroton X-ray scattering (Fratzl et al., 1997) have been used to investigate deformations of component collagen fibrils at the molecular level within a variety of tissue explants during quasi-static and dynamic loading. These highly sensitive techniques yield optical-based spectra that provide an indirect measure of the structural characteristics of collagen molecules and their packing. Analyses of these spectra under various mechanical loading conditions have provided insight into the molecular basis of the stress–strain response and viscoelastic behavior of collagenous tissues and have contributed to the development of a new model of collagen elasticity (Misof et al., 1997). Alternatively, small-angle light scatter has been recorded from tissue explants maintained in a native, hydrated state before and during biaxial loading to determine changes in collagen fiber orientation at the microscopic level (Billiar and Sacks, 1997). However, applicability of this technique is restricted to thin connective tissues such as cardiac valve leaflets and pericardium, and microstructural visualization again is limited to two dimensions. To acquire three-dimensional microstructural information from mechanically loaded tissue explants and engineered tissue constructs, the relatively new imaging technology confocal microscopy has been utilized. The confocal microscope provides a noninvasive means of collecting three-dimensional images from relatively thick specimens by forming a series of optical sections. Specifically, confocal microscopy has been used effectively in a fluorescence mode to evaluate three-dimensional changes in shape and volume of chondrocytes within labeled agarose gels and cartilage explants subjected to compressive forces (Guilak et al., 1995; Knight et al., 1998; Lee et al., 2000). To date, studies using this method have focused on the microstructural deformation of cells within loaded explants or scaffolds and have not included detailed microstructural analyses of the supporting matrix or scaffold.

In this article, we describe a new technique that allows structural–mechanical analyses of both cells and the supporting scaffold within mechanically loaded tissue constructs in

three dimensions. The technique involves the use of a highly modified uniaxial loading instrument in conjunction with a confocal microscope. A unique feature of this technique is the operation of the confocal microscope in a reflection (backscattered light) mode as a means to selectively visualize the microstructural deformation of the scaffold as well as any resident cells throughout the loading process. Because this imaging modality does not require fixation, staining, or physical sectioning, the response of the scaffold and any associated cells to various mechanical loads can be monitored over time within "live," fully hydrated specimens. In addition, vital (nontoxic) fluorochromes that label specific cellular attributes (e.g., membranes) may also be utilized to facilitate discrimination of cellular shape and volume or to monitor some relevant physiologic process (e.g., ion fluxes). The same experimental setup has been strategically adapted with optical prisms so that macroscopic deformation of the specimen in the width and thickness directions can be accurately quantified. The ability to visualize structural deformation of specimens at both macroscopic and microscopic levels during the application of controlled and quantified mechanical loads allows structural–mechanical relationships of biomaterials and cell–scaffold constructs to be accurately characterized from a tissue/construct level to a subcellular level of function.

In this study, the new mechanical loading–imaging technique was used to determine the structural–mechanical behavior of three different engineered tissue constructs: (1) a reconstituted type I collagen matrix, (2) a tissue-derived biomaterial known as intestinal submucosa, and (3) a tissue construct consisting of fibroblasts seeded within a reconstituted collagen matrix. Although both reconstituted collagen matrices and intestinal submucosa have been used *in vitro* to create tissue equivalents and *in vivo* as biomaterials for tissue repair and replacement, the structural–mechanical properties of these two types of scaffolds differ significantly and the structural–mechanical basis of the cellular response to these scaffolds is not fully understood. In this study, the new mechanical-loading method was used to visualize in four dimensions ($x$, $y$, $z$, and time) the load-induced deformation of the scaffold microstructure as well as to determine the engineering stress–strain and true stress–strain relationships. Finally, the evaluation of the structural–mechanical behavior of cells seeded within a reconstituted collagen matrix under load demonstrated the usefulness of this new technique for determining the microbiomechanical aspects of cell–scaffold interactions.

## Materials and Methods

### Sample Preparation

*Preparation of Three-Dimensional Collagen Matrix*

Native type I collagen prepared from calf skin by acid solubilization was obtained from Sigma Chemical Co. (St. Louis, MO) and dissolved in 0.01 M hydrochloric acid to achieve desired concentrations. To obtain a sterile preparation of collagen suitable for use as an *in vitro* scaffold for cells (see Preparation of Three-Dimensional Tissue Constructs below), the collagen solution was layered onto a volume (representing 10% of the collagen solution volume) of chloroform. Following incubation for 18 h at 4°C, the volume representing the collagen solution was removed, excluding the collagen solution–chloroform interface. The collagen solution was transferred to a sterile container and stored at 4°C prior to use.

Three-dimensional collagen matrices were prepared by neutralizing acid solubilized collagen with 10× phosphate-buffered saline (PBS) (ionic strength of 0.14 M and pH 7.4). The neutralized collagen solution was polymerized in a dog-bone-shaped mold as described previously (Roeder et al., 2002). In brief, the mold consisted of a glass plate and a piece of flexible silicone gasket. The gauge section of the mold measured 10 mm in length, 4 mm in width, and approximately 1.8 mm in thickness. Neutralized collagen solution (1 ml) was added to each mold and the mold was incubated at 37°C in a humidified environment. Polypropylene mesh was embedded in the ends of each collagen matrix to facilitate clamping during mechanical loading.

*Preparation of Three-Dimensional Tissue Constructs*

Three-dimensional tissue constructs were prepared by adding fibroblasts to the neutralized collagen solution immediately prior to polymerization. Swiss mouse 3T3 fibroblasts were obtained from American Type Culture Collection (ATCC; Manassas, VA). Cells were propagated in Dulbecco's modified Eagle's medium (DMEM) with 1.5 g/l $NaHCO_3$, 10% calf serum, 100 U/ml penicillin, 100 $\mu$g/ml streptomycin, and 2 mM L-glutamine. Fibroblasts were harvested in complete medium, collected by centrifugation, and added as the last component to the neutralized collagen solution at a concentration of $1 \times 10^4$ cells/ml. The tissue construct then was polymerized in a dog-bone-shaped mold within a humidified environment at 37°C as described above. Follow-

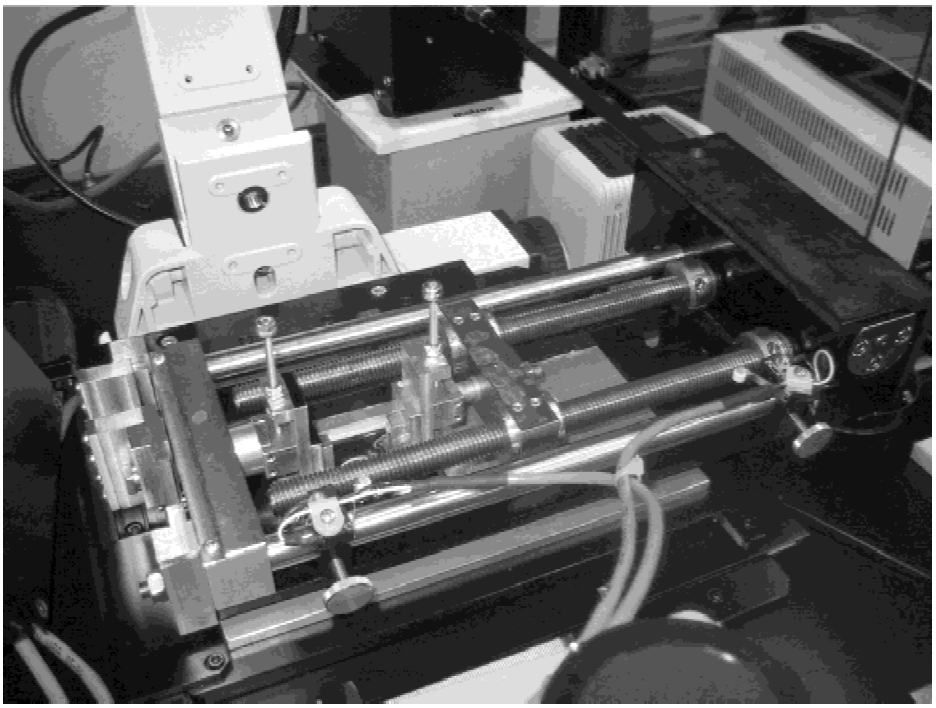

**Figure 1.** Photograph demonstrating the integration of a mechanical loading instrument with a laser scanning confocal microscope as a new means to perform microbiomechanical analyses of biomaterials and tissue constructs.

ing polymerization, tissue constructs were incubated in complete medium at 37°C in a humidified environment of 5% $CO_2$ in air for a minimum of 18 h prior to mechanical loading.

*Preparation of Tissue-Derived Biomaterial*

A tissue-derived biomaterial representing the submucosal layers of the porcine small intestine (known as intestinal submucosa) was obtained from Cook Biotech Inc. (West Lafayette, IN). For structural–mechanical analyses, the material was cut into a dog-bone shape with the same dimensions as specified for the reconstituted matrix and tissue construct.

## Mechanical Loading/Confocal Microscopy

The mechanical loading/confocal microscopy setup (Fig. 1) involved interfacing a highly modified Minimat 2000 miniature materials tester (Rheometric Scientific, Inc.; Piscataway, NJ) with a MRC 1024 laser scanning confocal microscope (BioRad; Hercules, CA) mounted on a Diaphot 300 microscope (Nikon Corp.; Tokyo, Japan). A specially designed adapter plate provided the physical connection between the Minimat and the confocal microscope (Fig. 2). This plate possessed a rectangular hole below which a coverglass was bonded, creating a well that allowed the samples to be tested in an aqueous environment representing physiologic temperature, pH, and composition. Optimal positioning of the specimen for confocal imaging was accomplished using clamps that offset the loading axis and

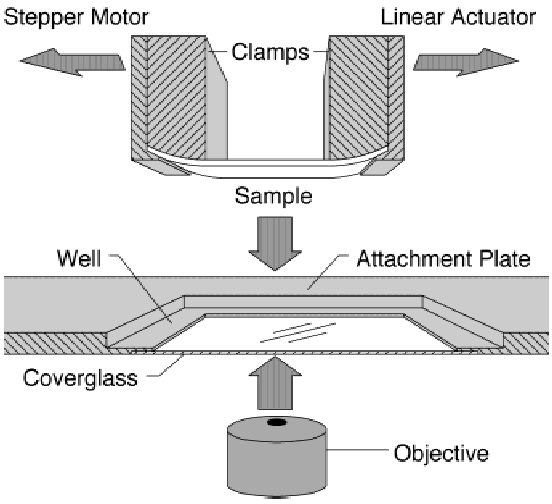


**Figure 2.** Schematic showing the interface between the mechanical loading instrument and the confocal microscope. An adapter plate provides the physical connection between the mechanical loading instrument and the confocal microscope and creates a well that allows specimens to be tested in an aqueous environment. Specially designed clamps offset the loading axis and hold the sample next to the coverglass.

maintained the specimen parallel with and close to the coverglass.

*Imaging*

Imaging of reconstituted collagen matrices, tissue-derived biomaterial, and tissue constructs during deformation-controlled loading was performed using the confocal microscope in a reflection and/or fluorescence mode. Reflection images were collected by equipping the confocal microscope with a 60×, 1.4 NA oil-immersion lens (Nikon) and a quarter-wave plate as described previously (Brightman et al., 2000). In brief, specimens were illuminated with 488-nm light generated by an Innova Enterprise argon-ion laser (Coherent Laser Group; Santa Clara, CA) and the reflected (back-scattered) light detected with a photomultiplier tube (PMT) using a blue reflection filter. Images representing a *z*-series (0.2 $\mu$m *z*-steps) of adjacent *x-y* scans were collected and compiled into either single-view overlay projections using Laser Sharp image-processing software (BioRad) or a three-dimensional projection using Voxel-View reconstruction software (Vital Images, Inc.; Plymouth, MN). When necessary, nonuniform background caused by interference and reflection from the optical path was removed using standard rank leveling procedures (Brightman et al., 2000). When the microscope was operated in a reflection mode, both the collagen fibril backbone of the scaffold and any resident cells could be visualized in three dimensions simultaneously.

To improve the resolution of collagen fibril structure and organization within dense biological specimens such as the tissue-derived biomaterial described here, specimens were stained with eosin (1 mg/ml) and visualized using confocal microscopy in a fluorescence mode. For these studies, an excitation wavelength of 488 nm was used and emission was detected using a 515-nm long-pass filter. These same excitation and emission wavelengths were used to collect the autofluorescence properties of an unstained specimen; however, in this case, resolving power was somewhat lower.

To enhance discrimination of cells from the surrounding collagen fibrils, tissue constructs were treated with the vital fluorochrome $DiOC_6(3)$ (1 mg/ml; Molecular Probes; Eugene, OR). In this way, reflected light from the collagen fibrils could be collected simultaneously with cell-based fluorescence. An argon-ion laser was used at 488 nm for excitation, and fluorescence from labeled cells was detected with a 515-nm long-pass filter. Both reflected light and fluorescence were collected along the same optical axis and separated immediately prior to entry into respective PMTs, thus allowing discrimination of fluorescence from the scattered light signal.

*Quantification of Mechanical Properties*

Tensile properties of reconstituted collagen matrices, tissue-derived biomaterials, and tissue constructs were measured by the modified Minimat 2000 miniature materials tester as previously described (Roeder et al., 2002). In brief, one end of each specimen was attached to a stepper motor-controlled linear actuator and the other end was attached to a load cell. Smooth clamp surfaces held the polypropylene mesh embedded in the ends of the reconstituted collagen matrices, which minimized stress concentrations due to clamping. For the tissue-derived biomaterial, mesh was not used, and the specimen was placed directly in the clamps. Additionally, to allow the specimen to be held close to the coverglass, the clamp surfaces were angled slightly away from the coverglass and the sample bent around a smooth curve (Fig. 2). For experiments involving reconstituted collagen matrices and tissue constructs, a specially designed load cell with a sensitivity of 0.0003 N was employed. Alternatively, a load cell with 0.01 N sensitivity was used for the tissue-derived biomaterial. For these studies, a strain rate of 10 mm/min was applied to all specimens; this rate is consistent with previous investigations on similar materials (Özerdem and Tözeren, 1995; Osborne et al., 1998). However, it should be noted that the mechanical behavior of reconstituted collagen matrices and other biological tissues is strain-rate dependent (Fung, 1993; Roeder et al., 2002). Phosphate buffered saline, pH 7.4, or complete culture medium was placed in the well of the adapter plate to provide an aqueous environment representing physiologic conditions during loading of the specimens.

The mechanical behavior of each specimen, including engineering stress ($\sigma_e$), true stress ($\sigma_t$), and strain ($\varepsilon$) were calculated from the load-displacement recordings. Strain was calculated as the change in length or cross-head displacement ($\Delta l$) divided by the original length ($l_0$):

$$\varepsilon = \frac{\Delta l}{l_0}.$$

Engineering stress was calculated as

$$\sigma_e = \frac{F}{A_0},$$

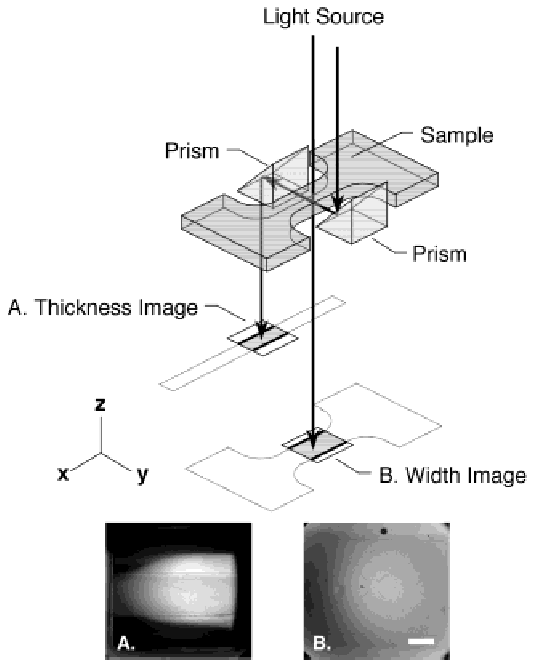


**Figure 3.** Schematic demonstrating visualization and quantification of specimen width and thickness for cross-sectional area determination during mechanical loading. Strategic placement of two right-angle prisms allowed collection of a low-power transmission image of a reconstituted collagen matrix in the *z* direction and quantification of specimen thickness (**A**). A low-power transmission image of the same specimen in the *y* direction allowed quantification of specimen width (**B**). Scale bar = 1 mm.

where $F$ was the force recorded by the Minimat and $A_0$ was the initial cross-sectional area (width × thickness) of the gauge section of the specimen. For calculation of true stress, the actual cross-sectional area of each specimen at a specific load was imaged, quantified, and substituted for $A_0$ in the above equation. More specifically, specimen width measurements during mechanical loading were made periodically during loading by collecting a low-power transmission image of the specimen in the *y* direction with the confocal microscope (Fig. 3B). For thickness measurements, right-angle prisms (Edmund Industrial Optics; Barrington, NJ) were strategically placed on each side of the specimen and used to collect a low-power transmission image of the specimen in the *z* direction (Fig. 3A). Incident light was reflected/bent 90° by the outer surface (hypotenuse) of the first prism and directed in the *y* direction. Reflected light was then bent 90° by a second prism and collected using a low-power objective. Based upon these width and thickness measurements, the cross-sectional area of the specimen at specified strain levels was quantified and used for calculation of true stress. Since collection of a *z*-series and corresponding width and thickness transmission images required several minutes, the tensile mechanical experiments were paused briefly to facilitate the imaging. However, load-displacement data was recorded continuously throughout the entire duration of the experiment.

## Results

### Structural and Mechanical Analysis in Three Dimensions

*Reconstituted Type I Collagen Matrix*

Previously, we and others have demonstrated that the three-dimensional microstructure of a reconstituted collagen matrix is an important determinant of its mechanical behavior (e.g., tensile and rheological properties), especially at the macroscopic level (Hsu et al., 1994; Roeder et al., 2002). Specifically, our laboratory showed that tensile mechanical properties of a collagen matrix, including the linear modulus and failure stress, were dependent upon fibril diameter, length, and density (Roeder et al., 2002). Unfortunately, these experiments provided no information regarding the way in which specific microstructures contributed to the three-dimensional distribution of mechanical loads (stress and strain states) throughout the specimen at the microscopic level during loading. In fact, such key structural–mechanical information is not readily available using traditional biomechanics methodologies established to date. In the present study, a new technique that integrates mechanical loading with confocal microscopy allowed changes in collagen fibril structure and organization within mechanically loaded reconstituted type I collagen matrices to be visualized in three dimensions (Fig. 4). In turn, time-lapse images collected from the same specimen at increasing loads could readily be constructed into a movie to facilitate visualization of the load-induced, three-dimensional microstructural deformation over time (http://www.cyto.purdue.edu/microanalysis/videos). Together, these results clearly demonstrate that upon loading, not only do component collagen fibrils become aligned in the loading direction, but the structure also becomes more compact. The observed reorientation of collagen fibrils within the reconstituted collagen matrix in the loading direction is consistent with the stretch-induced fibril and fibril bundle reorientation observed in explanted tissues, including mitral and aortic

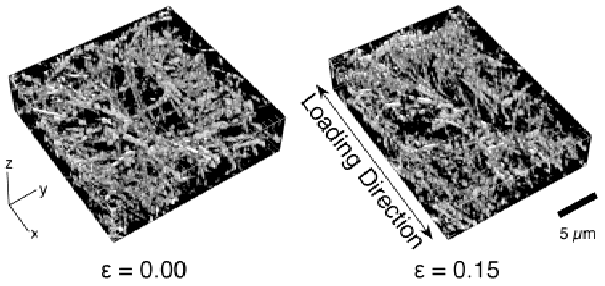


**Figure 4.** Three-dimensional reconstructed confocal reflection images show deformation of microstructure within a reconstituted collagen matrix (1.0 mg/ml type I collagen polymerized under physiologic conditions) under unloaded and loaded (applied strain level of 0.15 mm/mm) conditions.

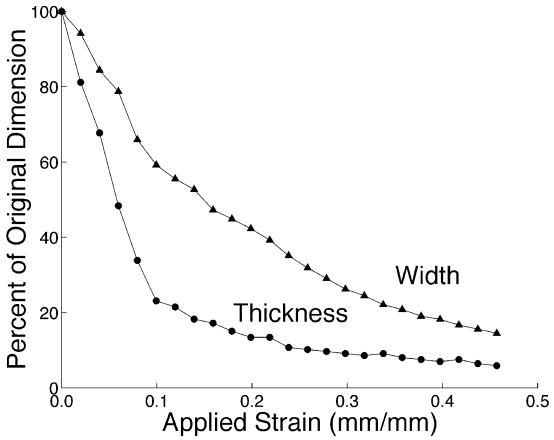


**Figure 5.** Width (▲) and thickness (●) measurements of a reconstituted type I collagen matrix (1.0 mg/ml type I collagen polymerized under physiologic conditions) at various levels of applied strain. Values are expressed as a percentage of original specimen dimensions (no applied strain).

valve leaflets (Clark and Finke, 1974; Broom, 1977; Billiar and Sacks, 1997), pericardium (Billiar and Sacks, 1997), and coronary artery (Bigi et al., 1981). In summary, the results of the present study provide the first visualization in four dimensions ($x$, $y$, $z$, and time) of the microstructural deformation experienced by a reconstituted collagen matrix under increasing load.

In addition to visualization of the three-dimensional microstructure of a reconstituted collagen matrix during loading, this new approach also facilitated the precise quantification of the macroscopic deformation imparted to the specimen in three dimensions as well as the associated force experienced by the specimen. Traditionally, such load-displacement data have been expressed in terms of engineering stress versus strain since accurate determination of specimen cross-sectional area during loading is difficult (Özerdem and Tozeren, 1995; Osborne et al., 1998). However, previous studies of the mechanical behavior of reconstituted collagen matrices and other biological materials have shown that these specimens experience substantial deformation not only in the loading direction but also in the lateral (width) and transverse (thickness) directions (Roeder et al., 2002). Such a change in specimen cross-sectional area during loading would mean that calculated engineering stress values would be significantly less than the true stress experienced by the specimen. The present technique provided a means for thickness and width measurements to be made throughout the loading process, thereby allowing determination of true stress. Figure 5 shows that with increased strain in the $x$ direction, the specimen decreases in the $y$ (width) and $z$ (thickness) directions. For the reconstituted collagen matrix, an applied deformation in the $x$ direction resulted in a nonlinear decrease in specimen width. On the other hand, a more rapid decrease in specimen thickness was noted up to a strain level of 0.1 mm/mm, after which the specimen approached a thickness representing approximately 5% of its original thickness up to the time of failure. The significance of this change in specimen cross-sectional area is evident upon examination of stress–strain properties of the collagen matrix expressed in terms of engineering stress and true stress (Fig. 6). From these results it is apparent that a substantial deviation occurs between true and engineering stress values as the level of strain increases. The most significant deviation was noted at failure, where true stress was approximately 50 times greater than engineering stress. Also evident in the stress–strain relationship are notched regions in the curves due to the brief interruptions in mechanical loading necessary for three-dimensional image collection. During this time, the reconstituted collagen matrix was maintained at a fixed extension (strain) and demonstrated a time-dependent decrease in stress, a phenomenon known as stress-relaxation. Stress-relaxation is one of several time-dependent mechanical (viscoelastic) properties exhibited consistently by biological specimens.

*Tissue-Derived Biomaterial*

The same technique was also applied to evaluate the micro-biomechanical properties of a tissue-derived biomaterial obtained from the submucosal layers of porcine small intestine representing an intact ECM. Load-induced changes in

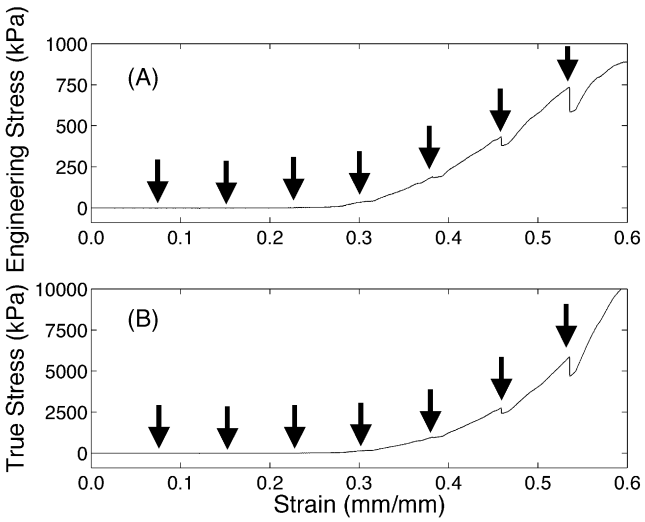


**Figure 6.** Stress–strain relationship of a three-dimensional ECM construct (1.0 mg/ml type I collagen polymerized under physiologic conditions) expressed in terms of engineering stress (**A**) and true stress (**B**). Arrows denote stress-relaxation response of the specimen due to an interruption in mechanical loading to accommodate image collection.

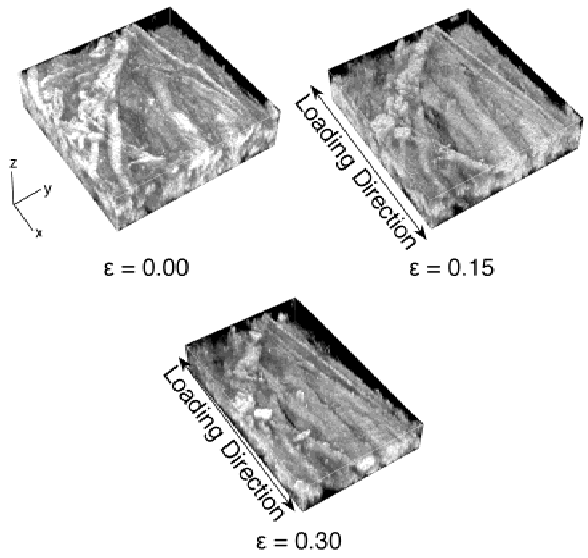


**Figure 7.** Three-dimensional reconstructed confocal reflection images show deformation of microstructure within the tissue-derived biomaterial under unloaded and loaded (applied strain levels of 0.15 mm/mm and 0.30 mm/mm) conditions.

the organization of component collagen fibrils within this biomaterial could be visualized using confocal microscopy in a reflection mode (Fig. 7). However, compared to the reconstituted matrix, resolving power was diminished due

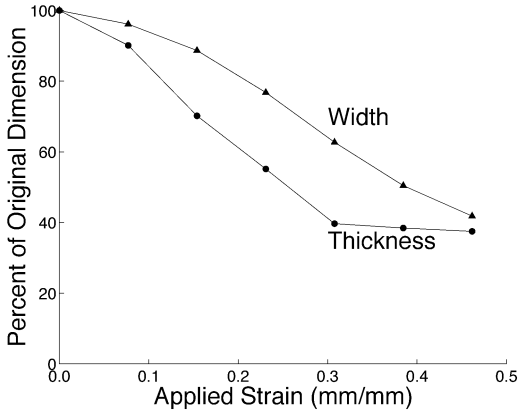


**Figure 8.** Width (▲) and thickness (●) measurements of a tissue-derived biomaterial at various levels of applied strain. Values are expressed as a percentage of original specimen dimensions (no applied strain).

to the specimen thickness and opacity. Image resolution could be enhanced by staining the matrix with eosin (data not shown). Unfortunately, the application of eosin as well as other commonly used collagen-staining dyes precludes the evaluation of "live" specimens, that is, tissue explants or tissue-derived biomaterials upon which cells have been seeded. In contrast to the reconstituted collagen matrix, the tissue-derived biomaterial exhibited a three-dimensional microstructure consisting of both individual collagen fibrils and organized bundles of fibrils. Upon loading, any "kinks" in fibrils or fibril bundles were removed as the fibrils became aligned in the loading direction (Fig. 7). Another characteristic of the load-induced fibril reorganization was the apparent shifting of selective fibrils and fibril bundles into different focal planes. As observed with the reconstituted collagen matrix, substantial deformations were demonstrated by the tissue-derived ECM biomaterial at the macroscopic as well as the microscopic level. With increased strain in the $x$ direction, the specimen showed decreases in both the $y$ (width) and $z$ (thickness) directions (Fig. 8). However, at a given strain level, the percent change in the width and thickness experienced by the intact biomaterial was less than that of the reconstituted collagen matrix. In fact, with increased applied strain, the biomaterial approached a thickness representing approximately 40% of its original thickness. Again the significance of the load-induced change in cross-sectional area is evident upon comparison of engineering stress versus true stress plotted as a function of strain (Fig. 9). It should be noted that the discrepancy between true versus engineering stress for the

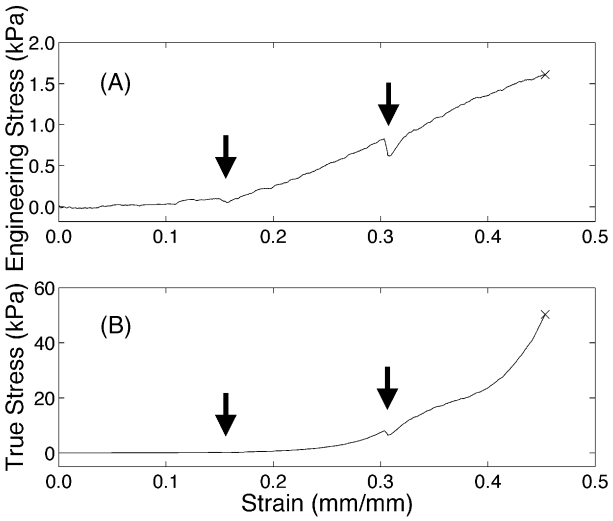


**Figure 9.** Stress-strain relationship of the tissue-derived biomaterial expressed in terms of engineering stress (**A**) and true stress (**B**). Arrows denote stress-relaxation response of the specimen due to an interruption in mechanical loading to accommodate image collection.

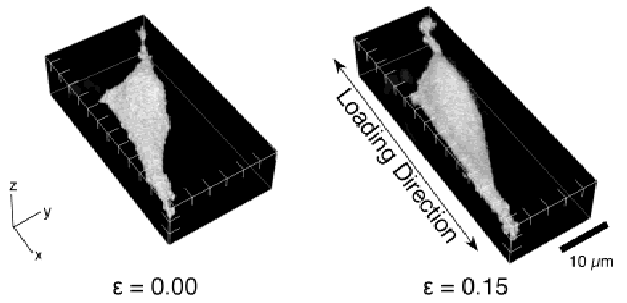


**Figure 10.** Three-dimensional reconstructed confocal images show deformation of a fibroblast within a three-dimensional tissue construct (collagen scaffold not shown) under unloaded and loaded (applied strain level of 0.15 mm/mm) conditions. To enhance discrimination of the cell from the surrounding collagen scaffold, cells were stained with the fluorescent membrane tracer dye $DiOC_6(3)$.

biomaterial is less than that observed for the reconstituted collagen matrix since the overall macroscopic deformation experienced by the biomaterial was less. Finally, as observed with the reconstituted collagen matrix, intestinal submucosa exhibited stress-relaxation during image collection due to its viscoelastic (time-dependence of mechanical properties) nature.

*Cell–Scaffold Interactions*

The integration of mechanical loading and confocal microscopy was also effective for studying the structural–mechanical aspects of cell–scaffold interactions. This technique was applied to a three-dimensional tissue construct consisting of a reconstituted collagen matrix seeded with fibroblasts. Both cell morphology and collagen fibril organization were visualized simultaneously in three dimensions within loaded specimens using confocal microscopy in a reflection mode. Again, for such three-dimensional analyses, no specimen processing was necessary and therefore multiple observations over time could be made on the same "live" specimen. To enhance the ability to discriminate three-dimensional cell morphology from the surrounding matrix, the tissue construct was treated with $DiOC_6(3)$, a vital fluorescent dye specific for cellular membranes. Figure 10 shows the deformation in three-dimensional cell shape and volume that occurred in response to a strain level of 0.15 applied to the tissue construct. These results show that the cell elongates and becomes oriented parallel to the direction of the applied load. This reorientation of cells is consistent with previous studies performed by Eastwood and coworkers (1998) in which tissue constructs were loaded, fixed, stained, and examined using routine light microscopy and stereomicroscopy.

## Discussion and Conclusions

The integration of mechanical loading with confocal microscopy provides a new tool that allows determination of the structural–mechanical properties of both reconstituted and tissue-derived three-dimensional matrices, especially at the microscopic level. A reconstituted collagen matrix and the ECM component of biological tissues represents a biphasic material consisting of insoluble fibrillar matrix surrounded by an interstitial fluid. As evidenced in Figure 4, only a portion of the total cross-sectional area of the reconstituted collagen matrix is represented by the fibrous matrix component. Therefore, the actual stress on component collagen fibrils is likely very different than the stress calculated at a macroscopic level since the force is assumed to be distributed across the entire cross-sectional area of the specimen. Therefore, the complex composition and structure of the ECM contribute to its characteristic heterogeneous and anisotropic mechanical behavior and provide the fundamental basis for the transition from macro- to microlevel mechanics. Imaging modalities such as reflection (backscattered

light) allow evaluation of specimens in an unprocessed ("native") and hydrated state. This approach eliminates structural artifacts that occur as a result of routine specimen processing prior to imaging via conventional methods. In addition, these imaging modalities allow specimens including cells (e.g., tissue explants or tissue constructs) to be maintained in a viable or "live" state. Long-term experiments involving specimens maintained at physiologic or experimentally controlled conditions could be readily accommodated by adapting the mechanical loading–imaging setup with an environmental chamber such that parameters including temperature, humidity, and carbon dioxide level can be controlled. Additionally, the adapter plate and clamps are manufactured from materials that can be readily sterilized so that specimens can be maintained under aseptic conditions.

Although the resolution of images obtained with confocal reflection microscopy appeared to decrease for specimens of increased thickness and opacity (e.g., tissue-derived biomaterial), it is plausible that image resolution of such specimens may be improved by adapting the mechanical loading instrument to a microscope with multiphoton excitation capabilities. Previously we have analyzed the collagen microstructure of intestinal submucosa based upon its autofluorescence properties (Voytik-Harbin et al., 2001). Although high quality autofluorescence images could be obtained with both confocal and multiphoton excitation, the imaging penetration depth obtained with multiphoton microscopy was greater than that obtained with confocal microscopy. An additional advantage of multi-photon-based imaging would be the enhanced second-harmonic-generated signal that these highly ordered biological components are able to generate.

The ability of this mechanical loading/confocal microscopy technique to obtain three-dimensional images which accurately reflect scaffold and cell microstructure in a native, unprocessed state provides the basis for precise quantification of structural as well as mechanical properties of the scaffold and any resident cells at a microscopic level. For example, the microstructural organization of component collagen fibrils within a reconstituted matrix can be quantified in terms of diameter, length, density, and orientation (Roeder et al., 2002). At the same time, if cells are present, three-dimensional qualitative information collected with the confocal microscope can be converted into quantifiable cell morphological parameters, including volume, surface area, and ellipticity. With the availability of vital fluorochromes specific for a broad range of cell-related processes, the biochemical status of the cell can also be monitored using the same experimental setup. The simultaneous acquisition of biochemical and structural–mechanical information during microbiomechanics studies will facilitate the identification of critical mechanisms involved in the transduction of mechanical stimuli into cellular responses. Based upon the Rayleigh criterion, the calculated resolution for our confocal system used in a reflection mode is 212 nm.

The ability to obtain accurate three-dimensional microstructural information of specimens under load is also critical to defining the states of stress and strain experienced by the scaffold and/or cells at a microscopic or local level. From consecutive three-dimensional images collected from tissue explants or constructs that were mechanically loaded over time, the three-dimensional distribution of local strains throughout the specimen can be experimentally measured at the microscopic level. At present, we are applying an algorithm based upon three-dimensional digital correlation techniques to automate the calculation of three-dimensional strain field distribution over time within mechanically loaded specimens. Precise definition of three-dimensional microstructural information will also allow the development of improved theoretical mechanical models that predict states of stress and strain at a microscopic level within loaded specimens. At present, predictive models of cell–scaffold biomechanics that are based on scaffold microstructure are limited by the assumption of a specific microstructural composition or by structural artifacts induced by the imaging techniques used to derive microstructural information (Farquhar et al., 1990; Schwartz et al., 1994; Wren and Carter, 1998; Soulhat et al., 1999; Agoram and Barocas, 2001).

In addition to providing qualitative and quantitative description of the deformation of specimens at a microscopic level, this mechanical loading/confocal microscopy technique allows specimen deformation to be quantified at a macroscopic level. The innovative placement of prisms allows images representing specimen thickness and width to be monitored throughout the loading process, thereby allowing calculation of true stress. This is important in the case of biological tissues in which true stress and engineering stress may be substantially different, since the latter assumes a constant cross-sectional area over which the load is acting. Another feature of this technique is the ability of the mechanical loading instrument to accommodate specimens representing a broad range of mechanical properties, including low-strength reconstituted collagen matrices and high-

strength biomaterials. By changing the configuration of the load cell on this specific instrument loads spanning six orders of magnitude (0.0001 N to 200 N) can be measured. Likewise, the specific mechanical loading instrument designed for these studies allows loads to be applied uniaxially in a tension or compression mode and supports quasi-static or dynamic loading formats. An attribute common to uniaxial loading instruments is that deformation is typically applied to only one end of the specimen. This asymmetric deformation results in movement of the original focal point within the specimen. However, realignment of three-dimensional images with respect to a single focal point for continuous visualization of load-induced deformation to cell and scaffold microstructure (see Video 1 at http://www.cyto.purdue.edu/microanalysis/videos) can be accomplished readily by identifying distinct structural entities within the specimen. Although image realignment can be performed manually, this process can be made more time efficient using digital volume correlation techniques (Bay et al., 1999). It should also be noted that this technique also requires that the mechanical loading of the specimen be briefly interrupted while the specimen is sectioned optically to obtain a detailed three-dimensional image. Because biological specimens demonstrate viscoelastic behavior, the initial stress generated by the application of a fixed extension decreases with time (stress-relaxation). The time period of interruption in the mechanical loading is determined by the amount of time required to collect a three-dimensional image and acquire images representing the specimen width and thickness. For the experimental setup and the imaging parameters (e.g., 512 × 512 pixels, 176 slices) used in these studies, the interruption time was approximately 15–20 min. Confocal microscopes with line-scanning or disc-scanning rather than point-scanning imaging technologies would likely minimize (although not eliminate) three-dimensional image-collection time and therefore the interruption in the extension process.

In conclusion, this new technique provides a means for determining critical quantitative and qualitative information regarding the structural and mechanical properties of the cellular microenvironment, as well as details of how specific scaffolds participate in the distribution of force from a macroscopic (tissue/construct) to a microscopic (cellular) level during mechanical loading of "live" specimens. Such fundamental biomechanics information will assist in the definition of fundamental principles and design criteria that will drive the next generation of tissue engineering strategies.

## Acknowledgments

The authors thank Kirk Foster for his technical assistance with the Minimat load cell modification, Bev Waisner for her assistance with tissue-culture-related aspects of this work, and Andrew O. Brightman and Gretchen Lawler for their editorial review of this work. This research was funded in part by an NSF Integrative Graduate Education and Research Training (IGERT) Program in Therapeutic and Diagnostic Devices (DGE-99-72770) and the Purdue University Vice President Academic Reinvestment Initiative entitled "Comprehensive Cell Biology Imaging and Analysis Facility." Blayne A. Roeder is an IGERT fellow.

## References

Agoram, B. & Barocas, V. (2001). Coupled macroscopic-microscopic modeling of fibrillar tissues and tissue equivalents. *J Biomech Eng* **123**, 362–369.

Bay, B.K., Smith, T.S., Fyhrie, D.P. & Saad, M. (1999). Digital volume correlation: Three-dimensional strain mapping using X-ray tomography. *Exp Mech* **39**, 217–226.

Bigi, A., Ripamonti, A., Roveri, N., Jeronimidis, G. & Purslow, P.P. (1981). Collagen orientation by X-ray pole figures and mechanical properties of media carotid wall. *J Mater Sci* **16**, 2557–2562.

Billiar, K.L. & Sacks, M.S. (1997). A method to quantify the fiber kinematics of planar tissues under biaxial stretch. *J Biomech* **30**, 753–756.

Brightman, A.O., Rajwa, B.P., Sturgis, J.E., McCallister, M.E., Robinson, J.P. & Voytik-Harbin, S.L. (2000). Time-lapse confocal reflection microscopy of collagen fibrillogenesis and extracellular matrix assembly in vitro. *Biopolymers* **54**, 222–234.

Broom, N.D. (1977). The stress-strain and fatigue behavior of glutaraldehyde preserved heart valve tissue. *J Biomech* **10**, 707–724.

Chen, C.S., Yannas, I.V. & Spector, M. (1995). Pore strain behaviour of collagen-glycosaminoglycan analogues of extracellular matrix. *Biomaterials* **16**, 777–783.

Chiquet, M. (1999). Regulation of extracellular matrix gene expression by mechanical stress. *Matrix Biol* **18**, 417–426.

Clark, R.E. & Finke, E.C. (1974). Scanning and light microscopy of human aortic leaflets in stressed and relaxed states. *J Thorac Cardiovasc Surg* **67**, 792–804.

Cowin, S.C. (2000). How is a tissue built? *J Biomech Eng* **122**, 553–569.

Eastwood, M., Mudera, V.C., McGrouther, D.A. & Brown, R.A. (1998). Effect of precise mechanical loading on fibroblast

populated collagen lattices: Morphological changes. *Cell Motil Cytoskeleton* **40**, 13–21.

Farquhar, T., Dawson, P.R. & Torzilli, P.A. (1990). A microstructural model for the anisotropic drained stiffness of articular cartilage. *J Biomech Eng* **112**, 414–425.

Fratzl, P., Misof, K. & Zizak I. (1997). Fibrillar structure and mechanical properties of collagen. *J Struct Biol* **122**, 119–122.

Fung, Y.C. (1993). *Biomechanics: Mechanical Properties of Living Tissues*, New York: Springer-Verlag.

Galbraith, C.G. & Sheetz, M.P. (1998). Forces on adhesive contacts affect cell function. *Curr Opin Cell Biol* **10**, 566–571.

Guilak, F., Ratcliffe, A. & Mow, V.C. (1995). Chondrocyte deformation and local tissue strain in articular cartilage: A confocal microscopy study. *J Orthop Res* **13**, 410–421.

Hsu, S., Jamieson, A.M. & Blackwell, J. (1994). Viscoelastic studies of extracellular matrix interactions in a model native collagen gel system. *Biorheology* **31**, 21–36.

Ingber, D. (1998). In search of cellular control: Signal transduction in context. *J Cell Biochem Suppl* **30–31**, 232–237.

Knight, M.M., Lee, D.A. & Bader, D.L. (1998). The influence of elaborated pericellular matrix on the deformation of isolated articular chondrocytes cultured in agarose. *Biochim Biophys Acta* **1405**, 67–77.

Lee, D.A., Knight, M.M., Bolton, J.F., Idowu, B.D., Kayser, M.V. & Bader, D.L. (2000). Chondrocyte deformation within compressed agarose constructs at the cellular and sub-cellular levels. *J Biomech* **33**, 81–95.

Misof, K., Rapp, G. & Fratzl, P. (1997). A new molecular model for collagen elasticity based on synchrotron X-ray scattering evidence. *Biophy J* **72**, 1376–1381.

Osborne, C.S., Barbenel, J.C., Smith, D., Savakis, M. & Grant, M.H. (1998). Investigation into the tensile properties of collagen/chondroitin-6-sulphate gels: The effect of crosslinking agents and diamines. *Med Biol Eng Comp* **36**, 129–134.

Ottani, V., Raspanti, M. & Ruggeri, A. (2001). Collagen structure and functional implications. *Micron* **32**, 251–260.

Özerdem, B. & Tözeren, A. (1995). Physical response of collagen gels to tensile strain. *J Biomech Eng* **117**, 397–401.

Roeder, B.A., Kokini, K., Sturgis, J.E., Robinson, J.P. & Voytik-Harbin, S.L. (2002). Tensile mechanical properties of three-dimensional type I collagen extracellular matrices with varied microstructure. *J Biomech Eng* **124**, 214–222.

Schwartz, M.H., Leo, P.H. & Lewis, J.L. (1994). A microstructural model for the elastic response of articular cartilage. *J Biomech* **27**, 865–873.

Soulhat, J., Buschmann, M.D. & Shirazi-Adl, A. (1999). A fibril-network-reinforced biphasic model of cartilage in unconfined compression. *J Biomech Eng* **121**, 340–347.

Viidik, A. (1972). Simultaneous mechanical and light microscopic studies of collagen fibers. *Z Anat Entwickl-Gesch* **136**, 204–212.

Voytik-Harbin, S.L., Rajwa, B. & Robinson, J.P. (2001). Three-dimensional imaging of extracellular matrix and extracellular matrix-cell interactions. *Meth Cell Biol* **63**, 583–597.

Wang, Y.N., Galiotis, C. & Bader, D.L. (2000). Determination of molecular changes in soft tissues under strain using laser Raman microscopy. *J Biomech* **33**, 483–486.

Wren, T.A.L. & Carter, D.R. (1998). A microstructural model for the tensile constitutive and failure behavior of soft skeletal connective tissues. *J Biomech Eng* **120**, 55–61.